



## Significance of Cuproptosis-related genes in immunological characterization, diagnosis and clusters classification in Parkinson's disease

Zhe Zhong<sup>1</sup>, Huiqing Wang<sup>1</sup>, Min Ye<sup>2\*</sup>, Fuling Yan<sup>1\*</sup>

<sup>1</sup>Department of Neurology, Affiliated ZhongDa Hospital, School of Medicine, Southeast University, Nanjing 210009, China

<sup>2</sup>Department of Neurology, Affiliated BenQ Hospital of Nanjing Medical University, Nanjing, 210019, China

### ARTICLE INFO

#### Original paper

#### Article history:

Received: June 12, 2023

Accepted: August 03, 2023

Published: November 30, 2023

#### Keywords:

Parkinson's disease; cuproptosis; immune infiltration; machine learning; predictive model

### ABSTRACT

Parkinson's disease (PD) is a progressive neurological disorder that affects millions of people throughout the world. Cuproptosis is a newly discovered form of programmed cell death linked to several neurological disorders. Nevertheless, the precise mechanisms of Cuproptosis-related genes (CRGs) in PD remain unknown. This study investigated immune infiltration and CRG expression profiling in patients with Parkinson's disease and healthy controls. Subsequently, we construct a predictive model based on 5 significant CRGs. The performance of the predictive model was validated by nomograms and external datasets. Additionally, we classified PD patients into two clusters based on CRGs and three gene clusters based on differentially expressed genes (DEG) of CRGs clusters. We further evaluated immunological characterization between the different clusters and created the CRGs scores to quantify CRGs patterns. Finally, we investigate the prediction of CRGs drugs and the ceRNA network, providing new insights into the pathogenesis and management of PD.

Doi: <http://dx.doi.org/10.14715/cmb/2023.69.12.20>

Copyright: © 2023 by the C.M.B. Association. All rights reserved.

### Introduction

Parkinson's disease (PD) is a rapidly growing disorder in the world and will affect 12 million people by 2024 (1). PD is now considered to be a multisystem disease characterized by movement disorders (bradykinesia, rigidity, and rest tremor) and non-motor disorders (depression, anxiety, fatigue) (2). The pathological hallmarks are the degeneration of dopaminergic neurons and the accumulation of misfolded  $\alpha$ -synuclein (3). It is clear that the rising prevalence of PD places a strain on families as well as society. However, given the clinical heterogeneity and pathological complexity of PD, there is a lack of satisfactory treatment and no effective prevention strategies (4). So It is essential to develop targeted interventions by further exploring the underlying mechanisms of their heterogeneity and complexity.

Copper is essential for growth and survival and widely involved in vital biochemical reactions such as energy production, redox, and neurotransmitter biosynthesis as a cofactor for conserved enzymes (5,6). A complex and sophisticated set of mechanisms regulates the homeostatic balance of copper. In addition, copper homeostasis dysregulation can result in cell death and is linked to neurodegenerative diseases (7). Cuproptosis, different from apoptosis, ferroptosis, and necroptosis, is a newly discovered form of programmed cell death. Recent studies have shown that Cuproptosis depends on mitochondrial respiration and that copper can directly bind to lipid components of the tricarboxylic acid (TCA) cycle, causing protein aggregation and dysregulation, and eventually inducing cell death

(8,9). Therefore, mitochondria play an essential role in Cuproptosis. It is important to note that mitochondrial dysfunction has a central function in PD progression (10,11). Thus, The correlation between cuproptosis-related genes (CRGs) and Parkinson's disease is significant for elucidating mechanisms of PD heterogeneity and complexity.

Recent research shows that cuproptosis may play a role in the development of some cancers and neurodegenerative diseases. Nevertheless, the role and immunologic characterization of cuproptosis have rarely been studied. Our study is systematically to explore the divergent expression of CRGs and immune features among normal and PD individuals. Furthermore, we develop a model for predicting the disclosure of patients by comparing 4 machine learning models. In addition, we classified PD patients into two clusters based on CRGs and three gene clusters based on differentially expressed genes (DEG) of CRGs clusters. We further evaluated immunological characterization between the different clusters and created the CRG scores to quantify CRGs patterns successfully. Lastly, we assess the prediction of CRGs targeted drugs and the ceRNA network, providing new perspectives on the pathogenesis and management of PD.

### Materials and Methods

#### Data acquisition and pre-processing

Six PD microarray datasets were downloaded from the GEO database: GSE8397 (GPL96 platform), GSE20292 (GPL96 platform), GSE20186 (GPL96 platform), GSE49036 (GPL570 platform), and GSE7621 (GPL570

\* Corresponding author. Email: [yemin1970@163.com](mailto:yemin1970@163.com); [15150655443@163.com](mailto:15150655443@163.com)

platform). We analyzed three array datasets based on the same platform including GSE8397, GSE202922, and GSE20186. These microarray data were processed and normalized by the "affy" package and removed batch effects with the "sva" package. A total of 49 substantia nigra with PD patients and 47 substantia nigra with healthy controls were included for further study. Additionally, two array datasets were combined as row external validation analysis, including the GSE49036 dataset (8 nigrostriatal samples from healthy controls and 15 nigrostriatal samples from PD) and the GSE7621 dataset (9 nigrostriatal samples from healthy controls and 16 nigrostriatal samples from PD). A dataset of 17 CRGs was obtained from previous related studies (5,9,12–14).

### Correlation analysis of CRGs with infiltration of immune cells

Single-sample gene set enrichment analysis (ssGSEA) was employed to evaluate the infiltration of immune cells in PD. We comprehensively assess every sample's immunologic characteristics based on 28 peripheral immune cell types in the ssGSEA algorithm. For each immune cell type, the relative abundance is indicated by the enrichment score taken from the ssGSEA analysis carried out by the R package (GSVA, GSEABase, and limma). Correlation coefficients between CRGs and infiltrated immune cells were analyzed. P-value < 0.05 was considered a significant correlation.

### Construction of a prediction model based on machine learning.

We used "caret" R packages to establish machine learning models including the Random Forest Model (RF), Support Vector Machine Model (SVM), Generalized Linear Model (GLM), and extreme Gradient Boosting (XGB) based on the CRGs. Furthermore, the residual distribution and feature importance were visualized in the "DALEX" package. We identify the Optimal machine learning model according to the relevant results. Subsequently, we used the top 5 significant variables as crucial PD-associated predictor genes. Receiver Operational Performance (ROC) curves were utilized to assess the diagnostic performance of the model and validate it with an external database.

### Construction of a nomogram model

We construct a nomogram model according to 5 predictive genes using the "rms" R package. We evaluate the predictive performance of the nomogram model using calibration curves and discriminant curve analysis (DCA). (15).

### Identification of molecular subtypes of CRGs

We classify individuals into different CRGs patterns according to 5 significant PD-associated predictor genes with the "ConsensusClusterPlus" package (16). We comprehensively evaluated optimal clusters according to the cumulative distribution function (CDF) curve, the consensus matrix, and the consistent clustering score (>0.9).

### Identification of CRGs-related DEGs between subtypes and functional enrichment analysis

The "limma" package is intended for selecting differentially expressed genes (DEGs) among different CRG patterns. These genes need to have adjusted p-values <0.05 as

well as fold changes >0.5. GSVA enrichment analysis was applied to explain the variations among different CRGs regarding gene enrichment biologically. Subsequently, we use "limma" R package to identify pathways and biological functions of differently expressed in GSVA scores. The condition about ( $|t| > 2, p < 0.05$ ) was considered as significantly altered.

### Estimation of the CRGs Gene Signature

The principal component analysis (PCA) algorithm computes each sample's CRGs scores and differentiates the CRGs-related patterns.

### Construction of drug network

Gene-targeted drug predictions were made using the Drug-Gene Interaction Database (DGIdb), and drug structure information was sought from the DrugBank database.

### Construction of ceRNA network

The mRNA-miRNA interaction pairs were predicted according to four databases: miRTarBase(<https://mirtarbase.cuhk.edu.cn>), miRDB(<https://mirdb.org>), and RNAInter(<http://www.rnainter.org/>), miRWalk3 (<http://mirwalk.umm.uni-heidelberg.de/>). Subsequently, we used the RNAInter to predict miRNA-lncRNA interaction pairs (confidence score >0.3) and finally constructed the ceRNA regulatory network. The ceRNA network was shown using Cytoscape (version 3.9.1).

### Statistical analysis

All analyses were conducted in R (version 4.20). Student's t-tests or Wilcoxon tests were employed to compare the two groups. The Kruskal-Wallis test was utilized to compare three groups. The Pearson correlation was assessed for correlation analysis. P<0.05 was considered statistically significant.

## Results

### Landscape of cuproptosis regulators and immune infiltration analysis in PD patients

The 'limma' package was employed to evaluate the differences in 17 CRGs' expression levels between PD patients and healthy controls. Eight significantly different CRGs (NFE2L2, FDX1, DLD, DLAT, PDHB, MTF1, GLS, and LIAS) were filtered and visualized with a heatmap and histogram (Figures 1A, B). NFE2L2 and MTF1 expression levels were higher than the control, whereas the expression levels of LIAS, DLAT, DLD, FDX1, PDHB, and GLS were significantly lower than controls. The chromosomal location of 17CRGs was visualized using the "RCircos" package (Figure 1C). To further explore whether CRGs have a critical function in PD, we explored the internal correlation of these differentially expressed CRGs. For example, DLD had a strong synergistic relationship with FDX1 (coefficient = 0.67) and DLAT (coefficient = 0.65), whereas MTF1 and NFE2L2 demonstrated antagonistic effects (coefficient = -0.46). (Figures 1E). Moreover, we further examined CRG correlation patterns and found that FDX1 and DLD were strongly associated with other regulatory factors. Figure 1D further illustrates the close relationship between these CRGs.

To determine immune system differences between PD and healthy controls, we use ssGSEA to perform immune

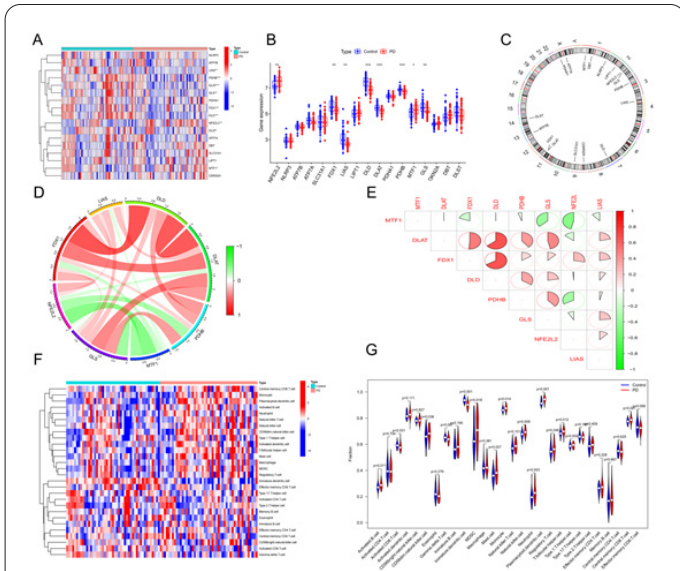


**Figure 1.** Landscape of cuproptosis regulators and immune infiltration analysis in PD patients. (A) The heatmap demonstrated the expression of 17 CRGs. \* $p < 0.05$ , \*\* $p < 0.01$ , and \*\*\* $p < 0.001$ . (B) Boxplots showed the expression of 8 CRGs in PD patients and healthy controls. (C) The chromosomal locations of 17 CRGs. (D) Gene relationship network diagram of 8 CRGs. (E) The area of the pie chart indicates correlation analysis of 8 CRGs. (F) The heatmap of 28 infiltrating immune cells. (G) The differences between immune cell infiltration levels in PD and non-PD controls.

infiltration analysis showing differences of immune cell types in PD versus controls (Figure 1F). The findings indicated that Activated.B.cells, CD56dim.natural.killer.cells, Mast.cel, MDSC, Monocyte, Natural.Killer.cells, Neutrophils, Plasmacytoid.dendritic.cell, T.follicular.helper.cel, Central.memory.CD8.T.cell, which was a high expression in PD patients, Activated.CD8.T.cel, Gamma.delta.T.cel, Immature.dendritic.cell was a low expression, showing that immune system alterations play a role in PD progression (Figure 1G). The results show that CRGs probably have a crucial function in the regulation of molecular and immunological infiltration of PD patients.

### Construction and assessment of machine learning models

We validated the differential CRGs in four machine-learning models (RF, XGB, SVM, and GLM) for the identification of high-diagnostic genes. We used the "DALEX" package to interpret and plot the distribution of residuals in the test set. The XGB model had the maximum area under the curve and relatively low residuals (AUC = 0.847 Figure 2A, B, D). Therefore, the XGB model is regarded as the most appropriate prediction model for PD. In the end, the top 5 most significant genes (MTF1, FDX1, NFE2L2, LIAS, and DLD) were chosen as the candidate genes for subsequent analysis (Figure 2C).

### Construction of the nomogram model and validation

We created a nomogram to predict the risk of Cuproptosis clusters based on five candidate genes. (Figure 3A). Moreover, DCA and calibration curves show the model's remarkable predictive ability. (Figure 3B, C). Then, we used an external combination data set of GSE49036 and GSE7621 to verify the prediction model. The optimistic performance in the test set (AUC = 0.784) (Figure 3D)

suggests that the diagnostic model is generally applicable.

### Correlation between CRGs and clinical PD

We further explore the correlation of CRGs expression levels with age and gender in PD patients. LIAS and age were negatively correlated ( $p = 0.001$ ), while NFE2L2 and age were positively correlated ( $p = 0.05$ ) (Figure 4B, C). In addition, FDX1 was more highly expressed in men ( $p < 0.041$ ) (Figure 4J). Other genes were not significantly correlated with Age and Gender (Figure 4A, D, E, F, G, H, I).

### Analyses of immune infiltration and functional enrichment in CRGs clusters

The relationship network diagram shows the close relationship between the five genes (Figure 1D). The cohort was separated into two groups: Cluster 1 ( $n = 26$ ) and Cluster 2 ( $n = 23$ ) based on consensus cluster analysis of 49 PD samples. The results showed that  $k = 2$  had the lowest intergroup differences and the CDF curve fluctuated in a minimal range (Figure 5A, B, C). PCA analysis showed that five different CRGs could completely distinguish between the two CRGs patterns (Figure 5D). First, we synthetically evaluated the expression of five CRGs among Cluster 1 and Cluster 2. Two CRGs patterns exhibit different CRGs expression landscapes (Figure 5E). The expression of NFE2L2 and FDX1 was higher in cluster 2 than in cluster 1., while MTF1 was the opposite. DLD and

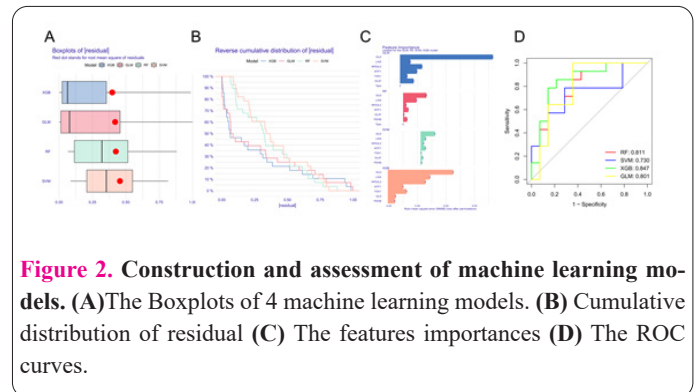


**Figure 2.** Construction and assessment of machine learning models. (A) The Boxplots of 4 machine learning models. (B) Cumulative distribution of residual (C) The features importances (D) The ROC curves.

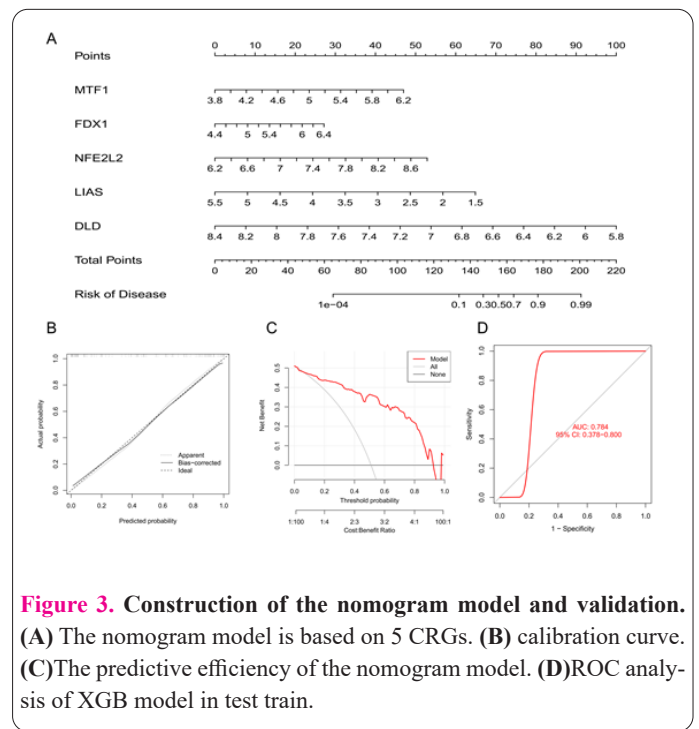


**Figure 3.** Construction of the nomogram model and validation. (A) The nomogram model is based on 5 CRGs. (B) calibration curve. (C) The predictive efficiency of the nomogram model. (D) ROC analysis of XGB model in test train.

DLAT were not significantly different between clusters 1 and 2 (Figure 5F). We used GSVA to understand the possible effects of these two clusters on biological behavior (Figure 5G). Cluster 1 was significantly enriched in immunological activation pathways such as Linoleic acid metabolism, Retinol metabolism, Cysteine and methionine metabolism, and drug metabolism, while cluster 2 was enriched in metabolism-related pathways like ErbB signaling pathway, Oxidative phosphorylation, and peroxisome.

We further assessed the role of CRGs in the immune microenvironment. The two clusters have significantly different immune cell infiltration (Figure 6A). Cluster 1 was associated with CD4+ T cell activation compared to cluster 2, suggesting that cluster 1 may be associated with autoimmune activation (Figure 6B). Further, in addition, the relationship between five CRG regulators and immune cells was assessed. The result revealed that DLD was significantly correlated with numerous immune B cells. (Figure 6C), so we assessed the immune cell infiltration of patients with high and low DLD levels. DLD was positively correlated with CD56bright.natural.killer.cell, Immature.dendritic.ce, Type.2.T.helper.cell, negatively correlated with Activated.dendritic.cell, CD56dim.natural.killer.ce, Mast.cel, Natural.killer.T.cell, Type.1.T.helper.cel(Figure 6D), suggesting immune function was weak in PD patients with high DLD expression.

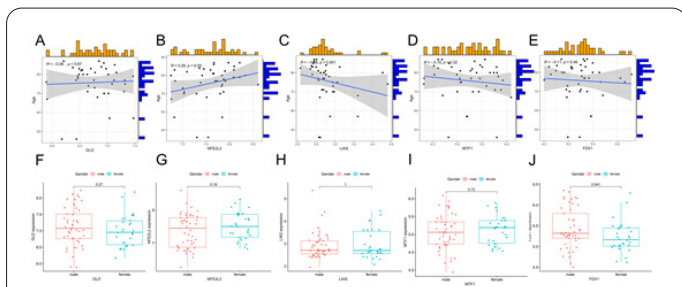


**Figure 4. Correlation Between CRGs and clinical in PD (A-E) Correlation between DLD. (A), NFE2L2 (B), LIAS(C), MTF1 (D), FDX1 (E), and age. (F–J) Correlation between DLD (F), NFE2L2 (G), LIAS(H), MTF1 (I), FDX1 (J), and Gender.**

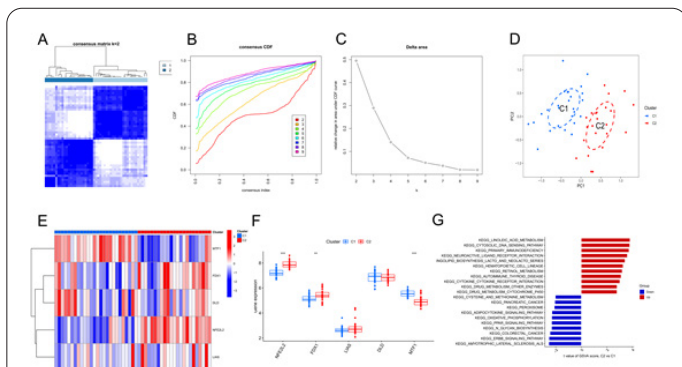


**Figure 5. Analyses of immune infiltration and functional enrichment in CRGs clusters. (A) Consensus matrices when k = 2. (B) consensus CDF. (C) Delta area. (D)Principal component analysis shows a remarkable difference in transcriptomes between the two CRG patterns. (E) The expression of 5 significant CRGs in Cluster1 and Cluster2. (F) The differential expression of 5 significant CRGs in Cluster1 and Cluster2. (G) The differences between Cluster1 and Cluster2 samples in the GSVA method.**

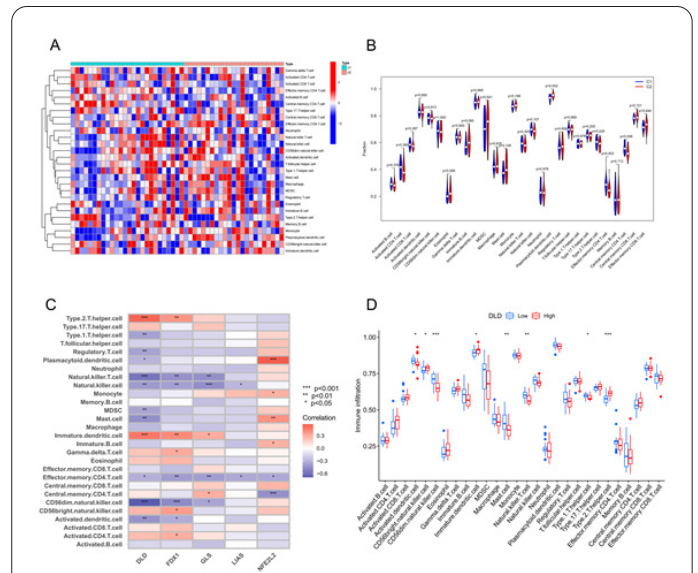


**Figure 6. Analyses of immune infiltration and functional enrichment in CRGs clusters. (A) The different expressions of 28 infiltrating immune cells between Cluster1 and Cluster2 were presented in the heatmap. (B) The differences between immune cell infiltration levels in cluster1 and cluster2 (C) The correlation with five significant CRGs and the immune cells. (D)The different expressions of infiltrating immune cells between high and low DLD expression groups.**

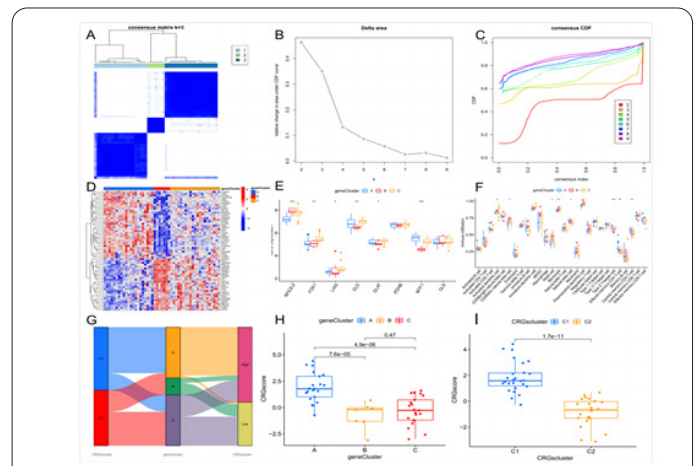


**Figure 7. Identification of gene patterns and development of the CRGs gene signature. (A) Consensus matrix when k = 3. (B) Delta area. (C) consensus CDF. (D)Expression heat map of the 64 CRGs-related DEGs in three gene patterns. (E) The different expression of 8 CRGs regulators in three gene patterns. (F) The different expression of infiltrating immune cells in three gene patterns. (G)The relationship between CRGs patterns, gene patterns, and CRGsscores in the Sankey diagram. (H)The variations in CRGs scores among gene Clusters. (I)The variations in CRGs scores among CRGs Clusters.**

### Identification of gene patterns and development of the CRGs gene signature

We employed a consensus clustering method to separate Parkinson's disease patients into gene patterns according to 64 CRGs-related DEGs (Figure S1). PD patients may be separated into three gene patterns (geneCluster A, B, and C) (Figure 7A-C). Figure 7D-E shows the DEG expression in the three gene groups. We discovered that the expression of CRGs and immune cell infiltration varied considerably between gene clusters. (Figure 7F). We used the PCA algorithms to compute five CRG scores per sample to quantify the gene pattern and compared the CRGs scores between CRGs patterns and gene patterns.

Figure 7G shows two CRG score groups, two CRGs patterns, and three CRGs gene patterns visualized in the Sankey diagram. CRG scores varied statistically significantly across CRG patterns. Cluster 1 had higher CRG scores than Cluster 2 (Figure 7I). Figure 7H displays that the highest CRG scores were geneCluster A, while there was no difference in geneCluster B and C.

**Prediction of marker gene-targeted drugs**

The interaction was analyzed using the DGIdb database to identify drugs targeting the marker genes. Figure 8 illustrates a visualization of the results by Cytoscape software. A total of 31 drugs targeted at markers genes were queried, of which 30 were NFE2L2 and 1 was MTF1. Unfortunately, we did not predict drugs targeting the remaining genes.

**Construction of ceRNA network**

We constructed a ceRNA network based on 5 marker genes from miRWalk3, miRDB, miRTarBase, and RNAInter. (Figure 9). Additionally, we discovered that 5 lncRNA (HCG27, HULC, TOB1-AS1, UCA1 and ZEB2-AS1) could bind hsa-miR-27b-3p to regulate FDX1, MTF1 and NFE2L2. In particular, hsa-miR-27b-3p was the only miRNA to regulate FDX1. For DLD, we found that 44 lncRNAs and 49 lncRNAs were able to regulate the DLD expression by competitively binding hsa-miR-106b-5p and hsa-miR-106a-5p. Of these, 44 lncRNAs were shared in the hsa-miR-106b-5p and hsa-miR-106a-5p. Meanwhile, hsa-miR-106-5p could also regulate other MTF1, LIAS, and NFE2L2. Thus, hsa-miR-106-5p played a crucial role in cuproptosis. In the ceRNA network of LIAS, a total of 13 lncRNA can bind hsa-miR-17-5p to regulate the gene. Moreover, hsa-miR-106-5p was also the key miRNA to regulate the other three genes. Details of ceRNA networks can be found in Figure 9.

**Discussion**

Parkinson's disease, common neurodegenerative disorder, is characterized by the loss of dopaminergic neurons in the substantia nigra. Recent evidence suggests that mitochondrial dysfunction is essential to the development of PD (17).

It was necessary for neurons with high energy demands for their survival and excitability, for dopaminergic neurons, this demand was even 20 times higher (18). Dopamine neurons were strongly dependent on mitochondrial aerobic respiration to produce ATP for energy, so the sub-

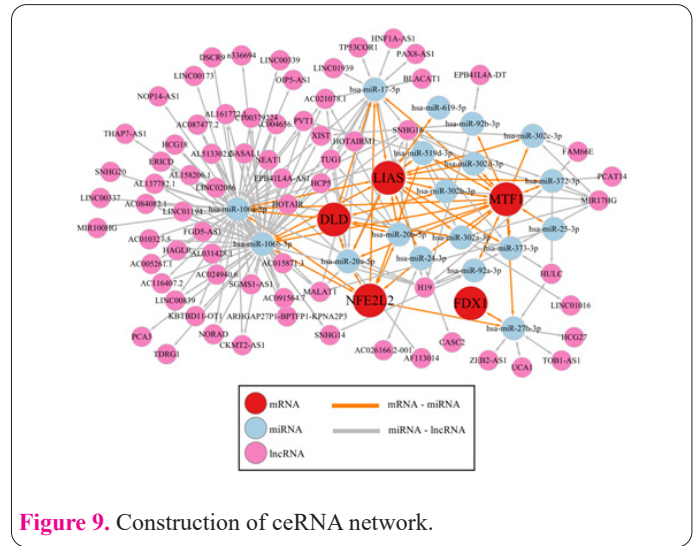


**Figure 9.** Construction of ceRNA network.

tantial metabolic demand was one of the fundamental reasons for their selective vulnerability to mitochondrial dysfunction(19,20). Additionally, Tsvetkov P (9) found a close correlation between cuproptosis and cellular mitochondrial respiration. Dopamine neuron cells are more susceptible to copper toxicity because mitochondrial respiration-dependent cells are 1000 times more sensitive to copper ionophores than glycolytic cells. Nonetheless, the precise mechanisms of cuproptosis in the regulation of PD have not yet been thoroughly investigated. A higher proportion of patients would be cured if the mechanisms and early prediction were investigated more. Therefore, we aimed to disclose additional potential mechanisms by elucidating the function about CRGs in the PD phenotype and immune microenvironment.

We performed a comprehensive analysis of CRG expression profiles in PD patients and healthy controls. CRGs may play a crucial role in the pathogenesis of PD based on the significant difference in CRG expression between PD patients and healthy controls. Next, we further evaluated the intercorrelation between CRG to elucidate the relationship between CRG and PD. Some CRGs were found to have obvious synergy or antagonism, as demonstrated by CRG interaction in patients with PD. Changes in immune cell abundance were observed between controls and PD patients. PD patients showed higher B-cell, neutrophil, NK cell levels, and MDSC infiltration, consistent with previously identified studies in blood or brain tissue (21–23).

In addition, we construct a high-accuracy prediction model by comparing the prediction performance of different machine models. Subsequently, we selected five significant variables (MTF1, FDX1, NFE2L2, LIAS, and DLD) from eight significant regulators of CRGs through the XGB-based model. MTF1 (Metal-responsive transcription factor 1) acts as a protector in the oxidative stress response of neuronal cells (24). Thus, MTF1, a key regulator of neurological cells, maybe a potential therapy choice for PD patients. FDX1 (Ferredoxin 1) and protein acetylation were crucial regulators of copper cell death(9), which was closely related to multiple basis metabolism (25). Our subsequent research will also investigate whether FDX1 depletion has a positive and beneficial function on clinical symptoms and neuronal protection in animal models of PD. NFE2L2 (nuclear factor, erythroid derived 2, like 2), as a mediator of inflammation and oxidative stress, played an important part in the development and mana-

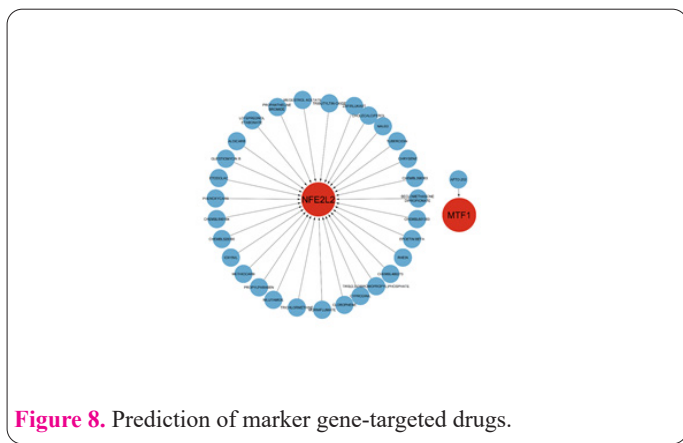


**Figure 8.** Prediction of marker gene-targeted drugs.

gement of PD. In addition, the role of NFE2L2 has been reported in the regulation of autophagy and acute and chronic neuroinflammation (26,27). LIAS(Lipoteichoic acid synthase) synthesizes mitochondria-related metabolic enzymes, energy metabolism and antioxidant responses (28). Several studies have demonstrated that LIAS mutations may result in complex metabolic diseases due to their association with mitochondrial energy metabolism (29). However, little correlation has been reported between LIAS and Parkinson's disease. DLD(dihydrolipoamide dehydrogenase), an NAD<sup>+</sup>-dependent oxidoreductase, functions in a number of mitochondrial complexes (30). In addition, DLD also can adhere to metal-oxide surfaces and bind DNA which leads to the apoptotic processes (31). In our study, DLD was correlated with several immune cells and more research is required to explore the correlation between DLD-mediated immune responses and PD. We used a combined external validation dataset (AUC = 0.784) to validate the predictive model. What's more, we established a nomogram model for diagnosing PD subtypes using MTF1, FDX1, NFE2L2, LIAS, and DLD. The model was shown to have a significant predictive effect and clinical application based on DCA curves.

In the early 1980s, McGeer (32) first noticed microglia activation and lymphocyte infiltration in PD patients. Since then, numerous studies found increased concentrations of pro-inflammatory cytokines in PD patients (33,34). Moreover, there are many changes in cellular immunity in the blood, including changes in the Platelet-to-lymphocyte ratio and neutrophil-to-lymphocyte ratio (35). There has been growing evidence that suggests that inflammation may have an essential part in the pathogenesis of PD. Our study identified two distinct molecular subtypes by the CRGs. Cluster 2 was highly linked to less memory. CD4.T.cell and had higher expression levels of FDX1, NFE2L2. It is acknowledged that memory.CD4.T.cell plays a central role in orchestrating adaptive immune responses. Based on our results, we proposed the following assumptions: 1. whether the decrease in memory CD4 T cells is linked with CRGs, 2. whether CRGs reduce the proliferative capacity of memory CD4 T cells or promote memory CD4 T cell death,3.whether the function of death is cuproptosis. We would conduct more experiments to explore the result.Then, three gene clusters were identified by the DEGs of the two CRGs clusters and the PCA algorithm used to calculate the CRGs scores to quantify the pattern of CRGs. We found that CRGs cluster 1 and gene cluster A showed a higher CRG score than other clusters.

Finally, we analyzed the CRGs-targeted drugs and the ceRNA network. For the MTF1, APTO-253 could selectively induce CDKN1A (p21) and promote G0-G1 cell-cycle arrest without producing myelosuppression (36). However, there were no reports of the function of neurological diseases. Cholecalciferol (Vitamin D3) was associated with NFE2L2, which was thought to be an essential factor in developing and regulating brain activity. It has been reported that PD had less VD3 than the control population in recent years. The evidence supported that VD3 presented anti-inflammatory and improved mitochondrial function in PD models (37,38). However, the role of VD3 in cuproptosis has not been clarified. Etodolac was the selective COX-2 inhibitor, which has been reported to affect anti-inflammation and oxidative stress (39). It was found to repair cognitive deficits in AD mice while

reducing A $\beta$  plaques, so it was a promising drug to treat neurodegenerative diseases (40). Non-coding RNA has an essential effect in PD development, miR-27b-3p, besides more, miR-106a-5p, miR106b-5p, and miR-17-5p were closely related to CRGs. Whether the role of gene-targeted drugs and non-coding RNA is unclear in PD, which needs more prospective studies.

There are several restrictions on our research. First, the data we used was only based on public sources; other, the more critical clinical samples (blood, tissue), which would confirm the prediction of the model and expression of CRGs were necessary. Furthermore, the potential association of CRGs with immunity needs to be further explored, especially the emphasis on the role of a single gene in the immune.

## Conclusion

Overall, our study systematically analyzed the role of CRGs and the infiltration of immune cells in patients with PD. Furthermore, we built a prediction model chosen from different machine learning models. Finally, we investigate the prediction of CRGs drugs and the ceRNA network. In summary, our study uncovered the importance of CRG, providing a meaningful foundation in PD diagnosis and personalized management.

## Declarations

### Ethics approval and consent to participate

Our study is based on open-access data, so there are no ethical issues and other conflicts of interest.

### Consent for publication

Not applicable.

### Author contributions

zz contributed to the writing and conceptualization of the manuscript, HQW contributed to figures and data. MY and FLY revised the content and format of the manuscript and made equally important contributions. All authors contributed to the article and approved the submitted version.

### Availability of data and materials

Publicly available data sets were analyzed in this study. The data can be found below: GEO, <https://www.ncbi.nlm.nih.gov/geo/>.

### Competing interests

The authors declare that the research was conducted in the absence of any commercial or financial relationships that could be construed as a potential conflict of interest.

## References

1. Dorsey ER, Sherer T, Okun MS, Bloem BR. The Emerging Evidence of the Parkinson Pandemic. *J Park Dis.* 2018;8(s1):S3–8.
2. Reich SG, Savitt JM. Parkinson's Disease. *Med Clin North Am.* 2019 Mar;103(2):337–50.
3. Tolosa E, Garrido A, Scholz SW, Poewe W. Challenges in the diagnosis of Parkinson's disease. *Lancet Neurol.* 2021 May;20(5):385–97.
4. Armstrong MJ, Okun MS. Diagnosis and Treatment of Parkinson Disease: A Review. *JAMA.* 2020 Feb 11;323(6):548–60.
5. Banci L, Bertini I, Cantini F, Ciofi-Baffoni S. Cellular copper distribution: a mechanistic systems biology approach. *Cell Mol Life*

- Sci CMLS. 2010 Aug;67(15):2563–89.
6. Baker ZN, Cobine PA, Leary SC. The mitochondrion: a central architect of copper homeostasis. *Met Integr Biometal Sci.* 2017 Nov 15;9(11):1501–12.
  7. Rae TD, Schmidt PJ, Pufahl RA, Culotta VC, O'Halloran TV. Undetectable intracellular free copper: the requirement of a copper chaperone for superoxide dismutase. *Science.* 1999 Apr 30;284(5415):805–8.
  8. Oliveri V. Selective Targeting of Cancer Cells by Copper Ionophores: An Overview. *Front Mol Biosci.* 2022;9:841814.
  9. Tsvetkov P, Coy S, Petrova B, Dreishpoon M, Verma A, Abdusamad M, et al. Copper induces cell death by targeting lipoylated TCA cycle proteins. *Science.* 2022 Mar 18;375(6586):1254–61.
  10. Grünewald A, Kumar KR, Sue CM. New insights into the complex role of mitochondria in Parkinson's disease. *Prog Neurobiol.* 2019 Jun;177:73–93.
  11. Eldeeb MA, Thomas RA, Ragheb MA, Fallahi A, Fon EA. Mitochondrial quality control in health and in Parkinson's disease. *Physiol Rev.* 2022 Oct 1;102(4):1721–55.
  12. Ren X, Li Y, Zhou Y, Hu W, Yang C, Jing Q, et al. Overcoming the compensatory elevation of NRF2 renders hepatocellular carcinoma cells more vulnerable to disulfiram/copper-induced ferroptosis. *Redox Biol.* 2021 Oct;46:102122.
  13. Aubert L, Nandagopal N, Steinhart Z, Lavoie G, Nourredine S, Berman J, et al. Copper bioavailability is a KRAS-specific vulnerability in colorectal cancer. *Nat Commun.* 2020 Jul 24;11(1):3701.
  14. Dong J, Wang X, Xu C, Gao M, Wang S, Zhang J, et al. Inhibiting NLRP3 inflammasome activation prevents copper-induced neuropathology in a murine model of Wilson's disease. *Cell Death Dis.* 2021 Jan 18;12(1):87.
  15. Iasonos A, Schrag D, Raj GV, Panageas KS. How to build and interpret a nomogram for cancer prognosis. *J Clin Oncol Off J Am Soc Clin Oncol.* 2008 Mar 10;26(8):1364–70.
  16. Wilkerson MD, Hayes DN. ConsensusClusterPlus: a class discovery tool with confidence assessments and item tracking. *Bioinform Oxf Engl.* 2010 Jun 15;26(12):1572–3.
  17. Malpartida AB, Williamson M, Narendra DP, Wade-Martins R, Ryan BJ. Mitochondrial Dysfunction and Mitophagy in Parkinson's Disease: From Mechanism to Therapy. *Trends Biochem Sci.* 2021 Apr;46(4):329–43.
  18. Mamelak M. Parkinson's Disease, the Dopaminergic Neuron and Gammahydroxybutyrate. *Neurol Ther.* 2018 Jun;7(1):5–11.
  19. Bolam JP, Pissadaki EK. Living on the edge with too many mouths to feed: why dopamine neurons die. *Mov Disord Off J Mov Disord Soc.* 2012 Oct;27(12):1478–83.
  20. Surmeier DJ, Obeso JA, Halliday GM. Selective neuronal vulnerability in Parkinson disease. *Nat Rev Neurosci.* 2017 Jan 20;18(2):101–13.
  21. Guan Q, Liu W, Mu K, Hu Q, Xie J, Cheng L, et al. Single-cell RNA sequencing of CSF reveals neuroprotective RAC1+ NK cells in Parkinson's disease. *Front Immunol.* 2022;13:992505.
  22. Chen S, Liu Y, Niu Y, Xu Y, Zhou Q, Xu X, et al. Increased abundance of myeloid-derived suppressor cells and Th17 cells in peripheral blood of newly-diagnosed Parkinson's disease patients. *Neurosci Lett.* 2017 May 1;648:21–5.
  23. Muñoz-Delgado L, Macías-García D, Jesús S, Martín-Rodríguez JF, Labrador-Espinosa MÁ, Jiménez-Jaraba MV, et al. Peripheral Immune Profile and Neutrophil-to-Lymphocyte Ratio in Parkinson's Disease. *Mov Disord Off J Mov Disord Soc.* 2021 Oct;36(10):2426–30.
  24. Talukder M, Bi SS, Jin HT, Ge J, Zhang C, Lv MW, et al. Cadmium induced cerebral toxicity via modulating MTF1-MTs regulatory axis. *Environ Pollut Barking Essex* 1987. 2021 Sep 15;285:117083.
  25. Tsvetkov P, Detappe A, Cai K, Keys HR, Brune Z, Ying W, et al. Mitochondrial metabolism promotes adaptation to proteotoxic stress. *Nat Chem Biol.* 2019 Jul;15(7):681–9.
  26. Lee DH, Park JS, Lee YS, Han J, Lee DK, Kwon SW, et al. SQSTM1/p62 activates NFE2L2/NRF2 via ULK1-mediated autophagic KEAP1 degradation and protects mouse liver from lipotoxicity. *Autophagy.* 2020 Nov;16(11):1949–73.
  27. Redox control of microglial function: molecular mechanisms and functional significance - PubMed [Internet]. [cited 2022 Dec 9]. Available from: <https://pubmed.ncbi.nlm.nih.gov/24597893/>
  28. Xu G, Yan T, Peng Q, Li H, Wu W, Yi X, et al. Overexpression of the Lias gene attenuates hepatic steatosis in *Leprdb/db* mice. *J Endocrinol.* 2021 Feb;248(2):119–31.
  29. Mayr JA, Zimmermann FA, Fauth C, Bergheim C, Meierhofer D, Radmayr D, et al. Lipoic acid synthetase deficiency causes neonatal-onset epilepsy, defective mitochondrial energy metabolism, and glycine elevation. *Am J Hum Genet.* 2011 Dec 9;89(6):792–7.
  30. Li R, Luo X, Wu J, Thangthaeng N, Jung ME, Jing S, et al. Mitochondrial Dihydrolipoamide Dehydrogenase is Upregulated in Response to Intermittent Hypoxic Preconditioning. *Int J Med Sci.* 2015;12(5):432–40.
  31. Shin D, Lee J, You JH, Kim D, Roh JL. Dihydrolipoamide dehydrogenase regulates cystine deprivation-induced ferroptosis in head and neck cancer. *Redox Biol.* 2020 Feb;30:101418.
  32. McGeer PL, Itagaki S, Boyes BE, McGeer EG. Reactive microglia are positive for HLA-DR in the substantia nigra of Parkinson's and Alzheimer's disease brains. *Neurology.* 1988 Aug;38(8):1285–91.
  33. Sandor C, Millin S, Dahl A, Schalkamp AK, Lawton M, Hubbard L, et al. Universal clinical Parkinson's disease axes identify a major influence of neuroinflammation. *Genome Med.* 2022 Nov 16;14(1):129.
  34. Magnusen AF, Hatton SL, Rani R, Pandey MK. Genetic Defects and Pro-inflammatory Cytokines in Parkinson's Disease. *Front Neurol.* 2021;12:636139.
  35. Madetko N, Migda B, Alster P, Turski P, Koziorowski D, Friedman A. Platelet-to-lymphocyte ratio and neutrophil-to-lymphocyte ratio may reflect differences in PD and MSA-P neuroinflammation patterns. *Neurol Neurochir Pol.* 2022;56(2):148–55.
  36. Duffy MJ, O'Grady S, Tang M, Crown J. MYC as a target for cancer treatment. *Cancer Treat Rev.* 2021 Mar;94:102154.
  37. de Siqueira EA, Magalhães EP, de Assis ALC, Sampaio TL, Lima DB, Marinho MM, et al. 1 $\alpha$ ,25-Dihydroxyvitamin D3 (VD3) Shows a Neuroprotective Action Against Rotenone Toxicity on PC12 Cells: An In Vitro Model of Parkinson's Disease. *Neurochem Res.* 2022 Sep 6;
  38. da Costa RO, Gadelha-Filho CVJ, de Aquino PEA, Lima LAR, de Lucena JD, Ribeiro WLC, et al. Vitamin D (VD3) Intensifies the Effects of Exercise and Prevents Alterations of Behavior, Brain Oxidative Stress, and Neuroinflammation, in Hemiparkinsonian Rats. *Neurochem Res.* 2022 Aug 26;
  39. Elfakhri KH, Abdallah IM, Brannen AD, Kaddoumi A. Multi-faceted therapeutic strategy for treatment of Alzheimer's disease by concurrent administration of etodolac and  $\alpha$ -tocopherol. *Neurobiol Dis.* 2019 May;125:123–34.
  40. Pauls E, Bayod S, Mateo L, Alcalde V, Juan-Blanco T, Sánchez-Soto M, et al. Identification and drug-induced reversion of molecular signatures of Alzheimer's disease onset and progression in AppNL-G-F, AppNL-F, and 3xTg-AD mouse models. *Genome Med.* 2021 Oct 26;13(1):168.